Energetics, Structures, and Phase Transitions of Cubic and Orthorhombic Cesium Lead Iodide (CsPbI₃) Polymorphs

Bin Wang, Novendra Novendra,[ID] and Alexandra Navrotsky*[ID]

Peter A. Rock Thermochemistry Laboratory and NEAT ORU, University of California Davis, Davis, California 95616, United States

Ⓢ *Supporting Information*

ABSTRACT: Cesium lead iodide (CsPbI₃) perovskite has shown great potential as a light absorbing material for solar cell applications. Despite intense research leading to increasing power conversion efficiency, a major problem concerning CsPbI₃ lies in the long term stability and interconversion between different CsPbI₃ polymorphs, a subject barely studied from the thermodynamic perspective. We report the formation enthalpies of two CsPbI₃ polymorphs, α and δ CsPbI₃, using a combination of room temperature solution calorimetry in dimethyl sulfoxide (DMSO) and differential scanning calorimetry. We show that both polymorphs are stable with respect to their binary halides and confirm that the α-phase is a high temperature polymorph, metastable under ambient conditions. This work sheds light on patterns in polymorphism, possible decomposition reactions, materials stability, and compatibility within halide perovskites and related systems. Thermodynamic instability near ambient temperature of functional perovskites may be a general phenomenon related to their vibrational density of states.

Inorganic halide perovskite (IHP) materials have captured broad research interests and shown increasing power conversion efficiency (PCE) in perovskite solar cells (PSC).[1−4] The generic formula for a 3D-structured inorganic halide perovskite is ABX₃, where A = Cs⁺, Rb⁺; B = Pb²⁺, Sn²⁺; and X = I⁻, Br⁻, and Cl⁻. Compared to hybrid organic–inorganic perovskites (HOIP) where A is usually methylammonium (CH₃NH₃⁺, MA⁺) or formamidinium (HC(CH₂)₂⁺, FA⁺), IHPs exhibit superior thermal and chemical stabilities under exposure to external humidity, oxygen and heat, which is rendered by the replacement of organic with intrinsically more stable inorganic cations.[4]

Among various inorganic halide perovskites, cesium lead iodide (CsPbI₃) draws special attention for its desirable bandgap, ease of synthesis and tunable optical properties.[1,5−7] Tremendous efforts have been devoted to the synthesis, modification and application of CsPbI₃ materials. Despite this, studies on the thermodynamic properties of CsPbI₃ materials remain scarce. Yet the underlying thermodynamic properties determine thermal and atmospheric stability, possible decomposition reactions, and materials compatibility.[8]

There appear to be several polymorphs within the cesium lead iodide system, whose interconversion and thermodynamic and thermal stabilities have not been well characterized.[1,9−11]

The one used as a light harvesting material in perovskite solar cells is α-CsPbI₃ (E_g = 1.73 eV, black), which adopts a cubic perovskite crystal structure (space group: $Pm\bar{3}m$). However, a nonperovskite, δ-CsPbI₃ with wide band gap (E_g = 2.82 eV, yellow) and orthorhombic crystal structure (space group: $Pnma$), was reported to be thermodynamically more stable below ∼320 °C. When exposed to ambient conditions, α-CsPbI₃ undergoes an immediate phase transition to its orthorhombic polymorph (δ-CsPbI₃). A spontaneous phase transition from δ- to α-CsPbI₃ was also reported when the temperature was ramped to ∼320 °C.[1,9,10] Thus, the α-phase appears to be the high temperature stable polymorph, but this hypothesis needs thermodynamic verification.

Here we report the formation enthalpies of α- and δ-CsPbI₃ polymorphs from lead iodide (PbI₂) and cesium iodide (CsI) using a combination of room temperature solution calorimetry and differential scanning calorimetry (DSC), confirming the energetic stability of both polymorphs with respect to their binary halide components and the energetic metastability of α-CsPbI₃ relative to the δ-phase. We propose some energetics—structure correlations in different polymorphs in perovskite-forming halide systems.

The schematic crystal structure and powder X-ray diffraction pattern of the synthesized orthorhombic δ-CsPbI₃ are shown in Figure 1, the latter confirming phase pure product. Structural details of δ-CsPbI₃, as well as those of α-CsPbI₃, are shown in Table 1.

The measured enthalpies of solution in dimethyl sulfoxide (DMSO) of δ-CsPbI₃ and constituent iodides are given in Table 2. The thermochemical cycle used to calculate enthalpy of formation is also shown. The formation enthalpy of δ-CsPbI₃ from binary iodides (PbI₂ and CsI) is significantly exothermic, −16.93 ± 0.87 kJ/mol, in contrast to the positive value for the hybrid perovskite MAPbI₃.[14] This more favorable formation enthalpy of CsPbI₃ indicates the greater stability rendered by the symmetrical, spherical Cs⁺ ion compared to the volatile MA⁺ ion due to its polarity and asymmetry. Indeed in general organic–inorganic hybrid perovskites are less thermodynamically stable than purely inorganic ones, giving the latter advantages in long-term use. Furthermore, the "yellow phase" with edge sharing polyhedra seems to be confined to the inorganic systems and does not appear to occur in the hybrid systems. This energetic stability is unlikely to be counteracted by entropy terms for formation from binary iodide constituents. Therefore, δ-CsPbI₃ is expected to have a
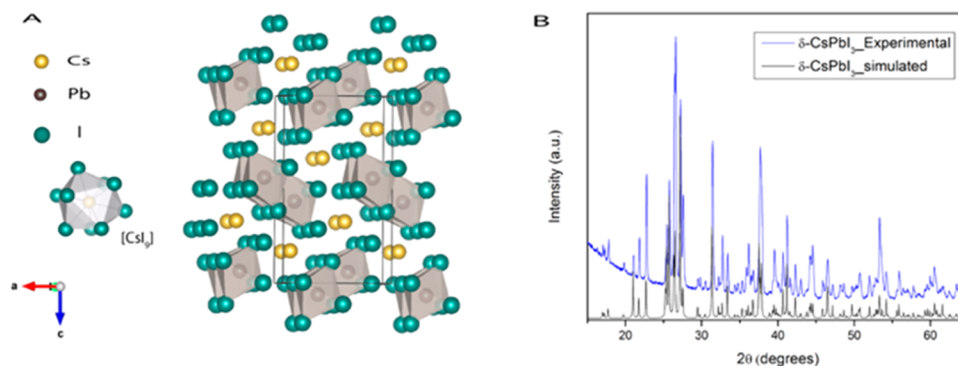
Figure 1. (A) Schematic crystal structure and (B) simulated and experimental powder X-ray diffraction patterns of δ-CsPbI$_3$.

Table 1. Structural Details of δ-CsPbI$_3$[a] and α-CsPbI$_3$[b]

CsPbI$_3$ Polymorph	Space group	Crystal system	Z	a	b	c	Density (g·cm^{-3})
δ-CsPbI$_3$	$Pnma$	Orthorhombic	4	10.4342(7)	4.7905(3)	17.7610(10)	5.3929
α-CsPbI$_3$	$Pm\overline{3}m$	Cubic	1	6.28940(19)	6.28940(19)	6.28940(19)	4.8111

[a]From ref 12. [b]From ref 13.

Table 2. Thermochemical Cycle to Calculate the Formation Enthalpies of α- and δ-CsPbI$_3$ at Room Temperature (25 °C)

Reaction Scheme[a]	Enthalpy Measurements	ΔH (kJ/mol)[b]	Note
δ-CsPbI$_3$ (xl, 25 °C) → PbI$_2$ (sln, 25 °C) + CsI (sln, 25 °C)	$\Delta H_1 = \Delta H_{sol}$ (δ-CsPbI$_3$, xl, 25 °C)	−46.12 ± 0.81 (8)	c
CsI (xl, 25 °C) → CsI (sln, 25 °C)	$\Delta H_2 = \Delta H_{sol}$ (CsI, xl, 25 °C)	−12.64 ± 0.21 (8)	c
PbI$_2$ (xl, 25 °C) → PbI$_2$ (sln, 25 °C)	$\Delta H_3 = \Delta H_{sol}$ (PbI$_2$, xl, 25 °C)	−50.41 ± 0.24 (8)	c
CsI (xl, 25 °C) + PbI$_2$ (xl, 25 °C) → δ-CsPbI$_3$ (xl, 25 °C)	$\Delta H_4 = \Delta H_f$ (δ-CsPbI$_3$, xl, 25 °C)	−16.93 ± 0.87 (8)	$\Delta H_4 = (-\Delta H_1) + \Delta H_2 + \Delta H_3$
δ-CsPbI$_3$ (xl, 25 °C) → α-CsPbI$_3$ (xl, 25 °C)	$\Delta H_5 = \Delta H_{\delta-\alpha}$ (CsPbI$_3$, xl, 25 °C)	14.10 ± 0.24 (4)	d
CsI (xl, 25 °C) + PbI$_2$ (xl, 25 °C) → α-CsPbI$_3$ (xl, 25 °C)	$\Delta H_6 = \Delta H_f$ (α-CsPbI$_3$, xl, 25 °C)	−2.83 ± 0.90 (4)	$\Delta H_6 = \Delta H_4 + \Delta H_5$

[a]State symbol: sln (DMSO solution), xl (crystalline solid). [b]The mean of values calculated from solution calorimetry or differential scanning calorimetry, unless otherwise specified. Uncertainty is two standard errors of the mean. Numbers of measurements indicated in parentheses. [c]Calculated from solution calorimetry. Temperature: 25 °C. Solvent: 25 g of 99.9% anhydrous DMSO. [d]Approximated to $\Delta H_{\delta-\alpha}$ (CsPbI$_3$, xl, 320 °C) from differential scanning calorimetry.

negative free energy of formation from its iodide components, which explains the long-term stability of δ-CsPbI$_3$ with no obvious decomposition or change in color or morphology when held in ambient conditions for months.

The black cubic perovskite phase (α-CsPbI$_3$), with a desirable band gap, transforms rapidly to δ-CsPbI$_3$ below ∼320 °C. Thus, α-CsPbI$_3$ can not be obtained for room temperature solution calorimetry. However, the thermodynamics of the phase transition from δ−α CsPbI$_3$ near 320 °C can be measured directly by differential scanning calorimetry (DSC), providing a means of relating the energetics of the two phases.

The DSC thermogram of δ-CsPbI$_3$ (Figure 2) shows an endothermic peak starting at 320 °C and centered at 325 °C, corresponding to the δ- to α-CsPbI$_3$ phase transition with an enthalpy change of 14.10 ± 0.24 kJ/mol. The entropy of transition is 14100/593 = 23.78 J/mol·K. By neglecting the difference in heat capacities between the two phases, these values can also be taken as a good approximation of the enthalpy and entropy of transition at ambient conditions. The heat capacity of the α-phase cannot be measured below the transition (as it does not exist), but the DSC curve (Figure 2) suggests a continuous curve could relate the heat capacity of the δ-phase below the transition and the α-phase above, supporting similar heat capacities. Similar heat capacities are expected as there are no phase transitions or disordering phenomena between 25 and 320 °C, and the vibrational heat
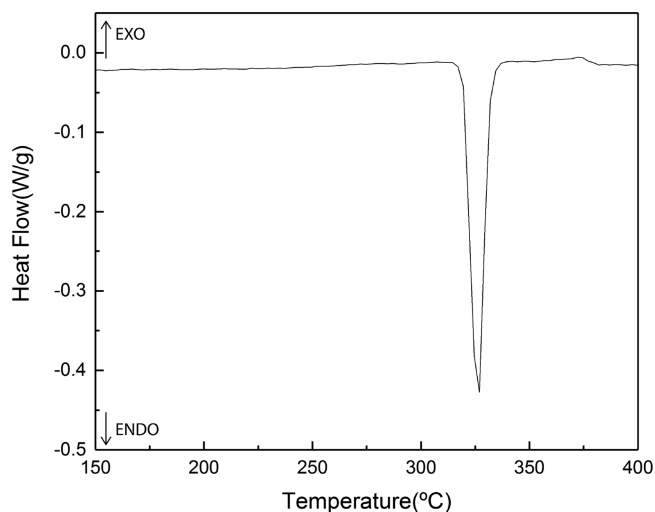

Figure 2. DSC thermogram of δ-CsPbI$_3$. Endothermic peak appears at 320 °C and centers at 325 °C

capacities of the two phases are expected to be similar in that range. With these approximations, the enthalpy of formation of the α-phase at ambient conditions is −2.83 ± 0.90 kJ/mol, making it just barely stable energetically. However, the large positive entropy of the δ−α transition clearly stabilizes α-CsPbI$_3$ above 320 °C. Thus, the δ-phase is confirmed to be

thermodynamically stable with respect to its binary iodides below 320 °C and the α-phase above that transition temperature. Because of the rapid reversibility of the transition, the α-phase with desirable solar cell applications is metastable and generally not attainable under ambient conditions.

The ideal cubic perovskite structure of α-CsPbI$_3$ consists of a three-dimensional network of corner-sharing BX$_6$ octahedra ($[PbI_6]^{4-}$) with the Cs$^+$ cation in the 12-fold coordination site formed in the middle of the cube of eight such octahedra.[15−17] δ-CsPbI$_3$ is not a perovskite. Its structure includes double chains of edge-sharing $[PbI_6]^{4-}$ octahedra linked by 9-fold coordinated Cs$^+$ cations (Figure 1A).[15−17] The edge-sharing $[PbI_6]^{4-}$ octahedra are tilted relative to the corner-sharing octahedra in α-CsPbI$_3$.[16] The difference in structures is manifested in the rather large enthalpy and entropy change associated with the $\alpha−\delta$ transition, much larger than those associated with typical distortional transitions in perovskites.[18,19] It is interesting that, despite such structural and energetic differences, the high temperature α-phase reverts rapidly to the δ-phase upon ambient cooling. The rapid reversibility suggests the possibility of a concerted, rather than reconstructive, mechanism for the transition, but this has not been investigated.

An analogous stability trend was observed in CsSnI$_3$, CsPbI$_3$'s tin counterpart, which undergoes a phase transition between orthorhombic and cubic polymorphs as temperature changes.[20] Likewise, cubic CsSnI$_3$ is a high temperature phase while the orthorhombic polymorph is a low temperature one, and a reversible displacive phase transition between the two polymorphs was reported. Yet there is no comprehensive investigation of CsSnI$_3$ from the energetics perspective, suggesting a potential subject for future research.

This octahedral tilting in the δ-phase CsPbI$_3$ may cause the band gap (E_g) to rise from 1.71 to 2.82 eV. Such octahedral tilting is not uncommon: in hybrid organic−inorganic perovskites, similar octahedral tilting and corresponding band gap increase were also widely observed.[21,22] Octahedral tilting was reported to reduce metal-halide orbital overlap, moving the valence band to lower energy and increasing the band gap.[21] However, since the δ-phase is not, strictly speaking, a perovskite, additional factors, including the edge-sharing of octahedra, may be important in determining the band gap.

Clearly, as manifested in the 320 °C phase transition, there is a thermodynamic competition between the high temperature α-phase (more symmetrical and higher enthalpy and entropy perovskite) and the low temperature δ-phase (structurally more complex and less symmetrical nonperovskite of lower enthalpy and entropy).

Such low temperature instability of perovskites relative to other phases may be a general phenomenon. Even within perovskites, transitions to more distorted polymorphs at lower temperature are common. Such distorted structures may have desirable properties resulting from their lower symmetry (including loss of a center of symmetry, leading, for example, to ferroelectric behavior, or they may compromise desirable band structure, as is the case for CsPbI$_3$. The distorted structures are of lower energy and lower entropy than the cubic aristotype, making the latter a high temperature polymorph. Similar arguments hold for stability relative to nonperovskite polymorphs. Such thermodynamic relations have been studied extensively in the context of high pressure geoscience, where MgSiO$_3$ based perovskite dominates the mineralogy of the Earth's lower mantle. This silicate perovskite is of higher enthalpy and entropy than polymorphs like MgSiO$_3$ ilmenite (which contains edge sharing polyhedra).[23] The reason for this behavior arises in large part from the vibrations of relatively loosely bound cations in the perovskite A-site which provide a large contribution to the low frequency vibrational density of states and lead to higher heat capacity and entropy.[23−26] The present study suggests similar behavior in halide perovskites. Future computational studies could address this phenomenon in CsPbI$_3$ perovskite despite the inability to maintain the perovskite at low temperature. It is also possible that cryogenic quenching in the absence of air and water vapor could preserve enough perovskite for experimental studies by low temperature heat capacity measurements, spectroscopy, and inelastic neutron scattering.

In summary, by using a combination of room temperature solution calorimetry and differential scanning calorimetry, we have obtained the enthalpies of formation of α- and δ-CsPbI$_3$, shown that both are stable with respect to their binary halides, and obtained the thermodynamics of the $\alpha−\delta$ transition. The desirable α-phase is metastable with respect to the δ-phase under ambient conditions. The effects of structural change on the thermodynamics and band gap have been discussed. The thermodynamic instability of perovskite phases at low temperature, reflecting their high vibrational entropy, may be a general phenomenon for halides as well as oxides.

■ ASSOCIATED CONTENT

Ⓢ Supporting Information

The Supporting Information is available free of charge on the ACS Publications website at DOI: 10.1021/jacs.9b05924.

> Experimental details of material synthesis, structural characterization, phase transition measurement, and solution calorimetry, thermal analysis (full pattern DSC and TG) plot (PDF)

■ AUTHOR INFORMATION

Corresponding Author
*anavrotsky@ucdavis.edu

ORCID Ⓞ
Novendra Novendra: 0000-0003-0927-5759
Alexandra Navrotsky: 0000-0002-3260-0364

Notes
The authors declare no competing financial interest.

■ ACKNOWLEDGMENTS

■ REFERENCES

(1) Swarnkar, A.; Marshall, A. R.; Sanehira, E. M.; Chernomordik, B. D.; Moore, D. T.; Christians, J. A.; Chakrabarti, T.; Luther, J. M. Quantum dotinduced phase stabilization of α-CsPbI$_3$ perovskite for high-efficiency photovoltaics. *Science* **2016**, *354*, 92.

(2) Zhang, W.; Eperon, G. E.; Snaith, H. J. Metal halide perovskites for energy applications. *Nat. Energy* **2016**, *1*, 16048.

(3) Hoffman, J. B.; Schleper, A. L.; Kamat, P. V. Transformation of Sintered CsPbBr$_3$ Nanocrystals to Cubic CsPbI$_3$ and Gradient

$CsPbBr_xI_{3-x}$ through Halide Exchange. *J. Am. Chem. Soc.* **2016**, *138*, 8603.

(4) Zhou, Y.; Zhao, Y. Chemical stability and instability of inorganic halide perovskites. *Energy Environ. Sci.* **2019**, *12*, 1495.

(5) Wang, K.; Jin, Z.; Liang, L.; Bian, H.; Bai, D.; Wang, H.; Zhang, J.; Wang, Q.; Liu, S. All-inorganic cesium lead iodide perovskite solar cells with stabilized efficiency beyond 15%. *Nat. Commun.* **2018**, *9*, 4544.

(6) Liang, J.; Wang, C.; Wang, Y.; Xu, Z.; Lu, Z.; Ma, Y.; Zhu, H.; Hu, Y.; Xiao, C.; Yi, X.; Zhu, G.; Lv, H.; Ma, L.; Chen, T.; Tie, Z.; Jin, Z.; Liu, J. All-Inorganic Perovskite Solar Cells. *J. Am. Chem. Soc.* **2016**, *138*, 15829.

(7) Xiang, S.; Fu, Z.; Li, W.; Wei, Y.; Liu, J.; Liu, H.; Zhu, L.; Zhang, R.; Chen, H. Highly Air-Stable Carbon-Based α-$CsPbI_3$ Perovskite Solar Cells with a Broadened Optical Spectrum. *ACS Energy Lett.* **2018**, *3*, 1824.

(8) Navrotsky, A. High-temperature oxide melt calorimetry of oxides and nitrides. *J. Chem. Thermodyn.* **2001**, *33*, 859.

(9) Eperon, G. E.; Paternò, G. M.; Sutton, R. J.; Zampetti, A.; Haghighirad, A. A.; Cacialli, F.; Snaith, H. J. Inorganic caesium lead iodide perovskite solar cells. *J. Mater. Chem. A* **2015**, *3*, 19688.

(10) Protesescu, L.; Yakunin, S.; Bodnarchuk, M. I.; Krieg, F.; Caputo, R.; Hendon, C. H.; Yang, R. X.; Walsh, A.; Kovalenko, M. V. Nanocrystals of Cesium Lead Halide Perovskites ($CsPbX_3$, X = Cl, Br, and I): Novel Optoelectronic Materials Showing Bright Emission with Wide Color Gamut. *Nano Lett.* **2015**, *15*, 3692.

(11) Waleed, A.; Tavakoli, M.; Gu, L.; Hussain, S.; Zhang, D.; Poddar, S.; Wang, Z.; Zhang, R.; Fan, Z. All Inorganic Cesium Lead Iodide Perovskite Nanowires with Stabilized Cubic Phase at Room Temperature and Nanowire Array-Based Photodetectors. *Nano Lett.* **2017**, *17*, 4951.

(12) Stoumpos, C. C.; Malliakas, C. D.; Kanatzidis, M. G. Semiconducting Tin and Lead Iodide Perovskites with Organic Cations: Phase Transitions, High Mobilities, and Near-Infrared Photoluminescent Properties. *Inorg. Chem.* **2013**, *52*, 9019.

(13) Trots, D. M.; Myagkota, S. V. High-temperature structural evolution of caesium and rubidium triiodoplumbates. *J. Phys. Chem. Solids* **2008**, *69*, 2520.

(14) Nagabhushana, G. P.; Shivaramaiah, R.; Navrotsky, A. Direct calorimetric verification of thermodynamic instability of lead halide hybrid perovskites. *Proc. Natl. Acad. Sci. U. S. A.* **2016**, *113*, 7717.

(15) Johnsson, M.; Lemmens, P. *Crystallography and Chemistry of Perovskites*; John Wiley & Sons, Ltd.: New York, 2007; p 11.

(16) Yuan, G.; Qin, S.; Wu, X.; Ding, H.; Lu, A. Pressure-induced phase transformation of $CsPbI_3$ by X-ray diffraction and Raman spectroscopy. *Phase Transitions* **2018**, *91*, 38.

(17) Sutton, R. J.; Filip, M. R.; Haghighirad, A. A.; Sakai, N.; Wenger, B.; Giustino, F.; Snaith, H. J. Cubic or Orthorhombic? Revealing the CrystalStructure of Metastable Black-Phase $CsPbI_3$ by Theory and Experiment. *ACS Energy Lett.* **2018**, *3*, 1787.

(18) Navrotsky, A. Thermochemistry of complex perovskites. *AIP Conf. Proc.* **2000**, *535*, 288.

(19) Navrotsky, A. Energetics and Crystal Chemical Systematics among Ilmenite, Lithium Niobate, and Perovskite Structures. *Chem. Mater.* **1998**, *10*, 2787.

(20) Chung, I.; Song, J. H.; Im, J.; Androulakis, J.; Malliakas, C. D.; Li, H.; Freeman, A. J.; Kenney, J. T.; Kanatzidis, M. G. $CsSnI_3$: Semiconductor or Metal? High Electrical Conductivity and Strong Near-Infrared Photoluminescence from a Single Material. High Hole Mobility and Phase-Transitions. *J. Am. Chem. Soc.* **2012**, *134*, 8579.

(21) Prasanna, R.; Gold-Parker, A.; Leijtens, T.; Conings, B.; Babayigit, A.; Boyen, H. G.; Toney, M. F.; McGehee, M. D. Band Gap Tuning via Lattice Contraction and Octahedral Tilting in Perovskite Materials for Photovoltaics. *J. Am. Chem. Soc.* **2017**, *139*, 11117.

(22) Lee, J.-H.; Bristowe, N. C.; Lee, J. H.; Lee, S.-H.; Bristowe, P. D.; Cheetham, A. K.; Jang, H. M. Resolving the Physical Origin of Octahedral Tilting in Halide Perovskites. *Chem. Mater.* **2016**, *28*, 4259.

(23) Ito, E.; Akaogi, M.; Topor, L.; Navrotsky, A. Negative Pressure-Temperature Slopes for Reactions Forming $MgSiO_3$ Perovskite from Calorimetry. *Science* **1990**, *249*, 1275.

(24) Wehinger, B.; Bosak, A.; Nazzareni, S.; Antonangeli, D.; Mirone, A.; Chaplot, S. L.; Mittal, R.; Ohtani, E.; Shatskiy, A.; Saxena, S.; Ghose, S.; Krisch, M. Dynamical and elastic properties of $MgSiO_3$ perovskite (bridgmanite). *Geophys. Res. Lett.* **2016**, *43*, 2568.

(25) Wentzcovitch, R. M.; Stixrude, L.; Karki, B. B.; Kiefer, B. Akimotoite to perovskite phase transition in $MgSiO_3$. *Geophys. Res. Lett.* **2004**, *31*, L10611.

(26) Akaogi, M.; Ito, E. Heat capacity of $MgSiO_3$ perovskite. *Geophys. Res. Lett.* **1993**, *20*, 105.